A Simulation Environment to Determine the Performance of SSA Systems

C. Kebschull
Institute of Space Systems, TU Braunschweig, Hermann-Blenk-Straße 23, 38108 Braunschweig
L. Reichstein
Institute of Space Systems, TU Braunschweig, Hermann-Blenk-Straße 23, 38108 Braunschweig
E. Stoll
Institute of Space Systems, TU Braunschweig, Hermann-Blenk-Straße 23, 38108 Braunschweig

ABSTRACT

Many states in Europe are participating in the build-up of an independent Space Situational Awareness (SSA) programme. One goal is to combine national assets like radar and telescope stations and share the data amongst the participating states. Within the EU and the ESA SSA programs have been setup to enable the collaboration between the different nation states. In order to get an idea of the capabilities of the different SSA system configurations the Institute of Space Systems (IRAS) has been developing a simulation software suite. Its main goal is to evaluate the performance of a given SSA system configuration. The paper outlines the architecture of the simulation software. Each integrated module necessary to achieve the complex simulation is described. A focus lies on the module to generate artificial Radar measurements, which are modelled on the microsecond time scale and the Orbit Determination (OD) module. The measurement generation module is able to generate noisy data. Based on variations like the noise level, the frequency of observation and the type of observed objects a sensitivity analysis is performed. The OD module is able to use different initial or statistical OD algorithms and configurations. Given the different levels of noise in the artificial measurements the achieved accuracies of OD configurations are analysed. The paper concludes with best practice recommendations for the use of different OD settings based on the chosen scenario.

1 INTRODUCTION

As Europe discovered the need for a capable Space Situational Awareness (SSA) system at the beginning of the last decade [17] different efforts have enabled the current developments within in the European Union (EU), European Space Agency (ESA) and several nation states to reduce the dependence on the United States. Among those programs, ESA's SSA Programme funded the development of software and infrastructure in periods 1 and 2 from 2009 till 2016. In the third period, which is envisaged to conclude in 2020 ESA's efforts go into further enhancing and integration of national assets [12]. Despite these cross-national efforts European nation states have been developing toward multiple independent SSA systems, motivated by the fact that ESA's purpose is "*[..] to provide for, and to promote, for exclusively peaceful purposes, [..]*", which excludes a military use of the developed capabilities [1], [17]. As a result several efforts have started in parallel to buildup SSA systems, like the CORrelation Tool (CORTO) cataloguing system by DEIMOS [8], the Spanish Space Surveillance and Tracking (S3T) [3] system, the German Space Situational Awareness Centre (GSSAC) building the German Experimental Space Surveillance and Tracking Radar (GESTRA) [22] and the German Space Operation Center (GSOC) [9] adding additional sensors to their network. In the light of these efforts several questions arise: Does every nation have enough access to the data needed to support their SSA operation? In the need of more data, does building new sensors or arranging cross-national agreements make more sense? In order to answer these questions in 2015 the IRAS has identified the need to create a simulation environment and has been developing the Radar System Simulator (RSS). Its purpose is to simulate an SSA system. Similar simulation environments exist, like the Space Object Observations and Kalman filtering (SPOOK) system [20]. Systems like RSS and SPOOK can be used to asses the performance or validate the working of an SSA system as mentioned in [4]. The RSS software suite enables to specify radar sensors as an input to a cataloguing backend. Given a population of

space objects and using the artificial data generated by the sensor simulation, an estimation can be made about the impact a sensor has on the cataloguing performance in terms of the overall catalogue size and timeliness or the fidelity of the stored orbital data. Furthermore, the OD algorithms and their configuration can be varied so that the impact of using a different method or configuration can be estimated as well. Within this paper the software suite to observe the impact of different OD methods and their settings. First the architecture of the RSS will be outlined in Sec. 2. More specifically the measurement generation will be described in Sec. 3. The OD methods that have been used to process the measurement data and the results will be shown in Sec. 4 and Sec. 5. Results from the different approaches are shown and compared. In Sec. 6 a conclusion and an outlook will be given.

2 SYSTEM ARCHITECTURE

The RSS software is divided into different tools. For this paper the following tools are used:

- MWG: Measurement generation
- SMART: OD algorithms
- PROCOR: Processes coordination
- CAT: Catalogue statistics

2.1 Messwertgenerator (MWG)

The measurement generator (german: Messwertgenerator) is able to derive synthetic measurements of radar sensors. The state of an object is represented by azimuth, elevation, range and, range-rate information. The user can specify multiple sensors, their location, and operation modes. The MWG currently offers the modes:

1. Mechanical Tracking,
2. Electronic Tracking and
3. Scanning.

While the first mode applies to mechanically steered antennas, the second and third correspond to phased array radars. The sensor configuration can be further refined by defining parameters like the sensor's Field of View (FOV), beam opening angle, wavelength, power, antenna transmit and receive gain, pulse repetition frequency, loss rate, false alarm probability, assumed measurement noise, and pulse integration settings. The underlying model derives the Signal-to-Noise Ratio (SNR) in addition to the state parameters for each observation. Measurement uncertainties (noise) are added with the root-means-square error

$$\sigma(M, SNR) = \frac{M}{\sqrt{2 \cdot SNR}}, \tag{1}$$

using the basic resolution M and the derived SNR per observation. Based on experience with the Tracking and Imaging Radar (TIRA) σ is further refined for observations that have a SNR above a reference (SNR_{ref}), where σ is considered a constant value σ_{ref}:

$$\sigma(M, SNR) = \begin{cases} \dfrac{M}{\sqrt{2 \cdot SNR}} & \text{, if } \; SNR < SNR_{ref} \\ \sigma_{ref} & \text{, if } \; SNR \geq SNR_{ref} \end{cases} . \tag{2}$$

The underlying radar performance model is called OVER and has been developed by Fraunhofer FHR [11]. The time steps used in the MWG simulation are variable to the needs of the sensor's definition of the pulse repetition frequency. In order to derive each observation, evaluate its SNR and uncertainty at the time needed the time steps can be at the order of milliseconds, when a pulse repetition frequency of 100 Hz is requested. The position of the target object and the sensor station have to be updated accordingly. As the MWG relies on the numerical propagator NPI Ephemeris Propagation Tool with Uncertainty Extrapolation (NEPTUNE) to extrapolate the state of the objects it is computationally expensive to this for each requested

time step, especially when larger populations are used as input for the simulation, like the MASTER-2009 population, which can contain up to 700 000 centimeter sized objects. NEPTUNE propagates the population over a time interval of several orbit revolutions. For the millisecond time steps a Chebyshev interpolation technique is used to retrieve the state of the objects [6]. The OVER model then evaluates in each time step whether the object is in the FOV and detectable, based on the derived SNR, false-alarm-rate and a random number generator. The MWG then creates corresponding output for time steps in which an object has been detected. *Detections* of the same object in one pass over a single sensor are grouped into *tracklets*. The output is written either to a text file or directly into a database, from where the processing chain starts to process the detections using OD algorithms.

2.2 Sophisticated Module for Analysis of Radar Tracklets (SMART)

The SMART tool retrieves tracklets and the corresponding detections from the database and processes them using different OD techniques. For Initial Orbit Determination (IOD) requests the tool can be configured to use either

- Gibbs, or
- Herrick-Gibbs

method as described in [21] and implemented and tested in [19]. For statistic OD SMART relies on the following methods:

- Weighted Least Squares (WLS),
- Extended Kalman Filter (EKF), and
- Unscented Kalman Filter (UKF).

They have been implemented and tested in [13] and [15]. The NEPTUNE propagator is at the core of the tool to extrapolate a state and covariance from an object catalogue to the epoch of the measurement. SMART is able to run in parallel with multiple instances accessing the database and processing tracklets as they are uploaded.

2.3 Process Coordinator (PROCOR)

The PROCOR tool manages the SMART instances and can configure them using configuration presets. Based on the incoming tracklets the tool creates processes and distributes them to the running SMART instances. A process is considered a task or job, which can be distributed to a processing instance, like SMART, in which case the process involves to apply OD algorithms to update or derive a new orbit. PROCOR makes sure that the tracklets are correlated to objects in the catalogue. Based on the kind of orbit PROCOR can choose from a range of configurations stored in the database and add it to the process, which is handed over to the SMART instance. These configurations can include OD and also propagator settings. Fig. 2.1 shows an overview of the data flow.

2.4 Catalogue Analysis Tool (CAT)

To be able to asses the catalogue status the tool CAT can access the database and derive statistics about the overall timeliness and accuracy of the object catalogue. In the sense of evaluating the setup of an SSA system individual objects can be monitored. The ephemeris derived through the OD algorithms in SMART can be compared to the *truth* known by the MWG and passed on for that purpose to the database. CAT compares the difference between the true and the derived state in the satellite centered coordinate frame UVW [16] or also referred to as RSW in [21], expressing the error in radial, along-track and cross-track components. It can also test whether the covariance related to the state properly reflects the uncertainty introduced from measuring, extrapolating and processing the data, when a gaussian error distribution is assumed. Furthermore, the output of the tool lets the user correlate data from the measurement directly to the created ephemeris, like the residuals, signal-to-noise ratio or part of the orbit the orbit was on, when the measurements were taken. An additional way to interpret the data in the object catalogue is the program Display of Object Circulating in Terrestrial Orbits (DOCTOR), which can visualize the objects in a 3D representation of the Earth orbits [18].

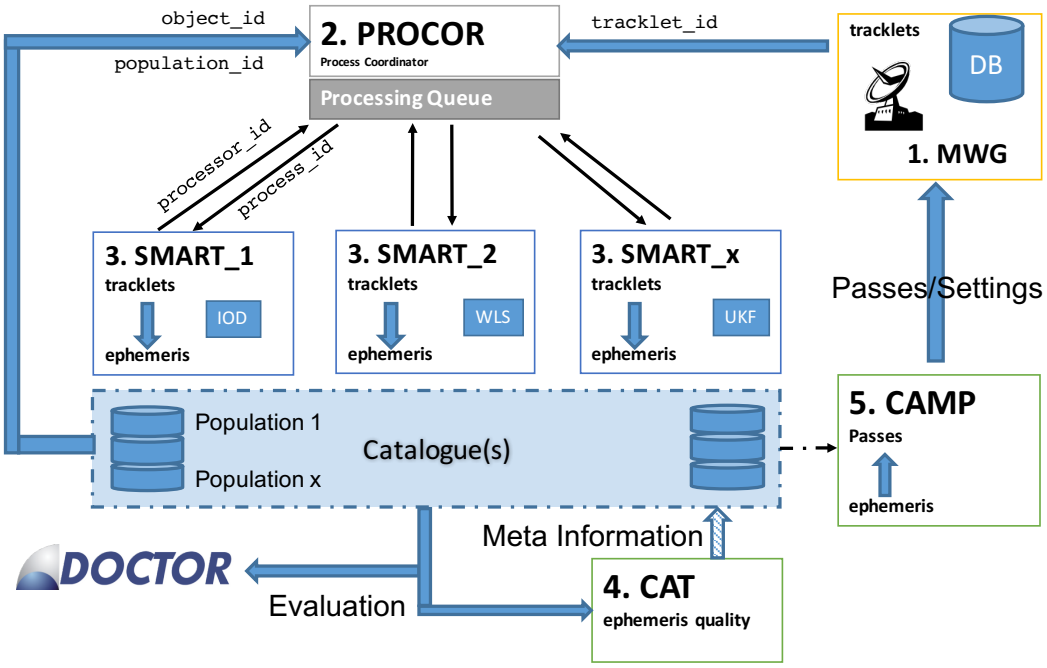

Fig. 2.1. A schematic of the process flow within the simulation environment.

2.5 Catalogue Maintenance and Pass prediction tool (CAMP)

The fifth tool in the chain closes the loop to the sensors. CAMP screens the object catalogue and creates pass predictions for objects crossing the local horizon of registered sensor stations. The passes are created using the estimated epoch, range, range-rate, azimuth and elevation information. In addition CAMP has a mode, where close approaches can be predicted. CAMP also uses the numerical propagator NEPTUNE. Within this paper however the tool is not directly used, as the MWG is put into auto-tracking mode, in which an object is centered exactly in the radar beam for the time of the crossing.

2.6 Tool communication

The communication between the tools is coordinated via the database. The underlying database is PostgreSQL v9.4+ [2]. It contains tables of the object catalogue but also tracklets, detections and tables containing configuration presets. PROCOR oversees the process distribution. SMART instances register at the database and receive a new *processor_id*. Each *processor_id* is associated with a *process_id* in the *Processesing Queue* table (cp. Fig. 2.1). When the tools are waiting for new processes they are polling the database,. PROCOR creates processes from tracklets that are coming in. It can be configured to run as a daemon in the background and wait for new tracklets to appear in the tracklets table. The user can also use it as a stand-alone application, specify tracklets directly and associate a custom configuration.

2.7 NPI Ephemeris Propagation Tool with Uncertainty Extrapolation (NEPTUNE)

NEPTUNE is a numerical propagator and has been developed at the IRAS between 2012 and 2015 as part of the Networking/Partnering Initiative (NPI) programme [7]. It uses a Störmer-Cowell integration routine [5], which uses a variable and multi-step, double integration. It also regards error correction for shadow boundary transits. NEPTUNE regards relevant force models, like [6]:

- EIGEN-GL04C, EGM96 and EGM2008 gravity models,
- NRLMSISE-00 and HWM07 to estimate the drag on Low Earth Orbit (LEO),
- Sun and Moon third-body perturbations,

- Solar Radiation Pressure (SRP),
- visible and infrared albedo,
- IERS solid and ocean tides,
- and the IAU 2006/2000A (GCRF/ITRF) transformations regarding Earth Orientation Parameters (EOP).

NEPTUNE is used through out the RSS tool suite, where an extrapolation of the state or covariance is needed. For the work in this paper the settings in Tab. 2.1 have been used. The different configurations between the tools introduces an additional modeling error, which reflects that the used force models in the propagator are unable to perfectly reflect the reality. As the MWG is considered to create the *truth* in the simulation environment, a reduced force model for the OD seems reasonable.

Table 2.1. Configuration of the numerical propagator for the tools used.

Force Model	MWG	SMART
EIGEN-GL04C	36×36	12×12
NRLMSISE-00, HWM07	☒	☒
Luni-solar	☒	☒
Solar Radiation Pressure (SRP)	☒	☒
Solid tides	☒	☒
Ocean tides	-	-
Earth Orientation Parameters (EOP)	-	-

3 MEASUREMENT GENERATION

For the generation of measurements using the MWG, first the initial population needs to be defined. The population can originate from Two Line Elements (TLE) records or the MASTER-2009 population [10]. For this paper five space objects and their orbits are defined. Tab. 3.1 shows the orbital parameters. Three objects (3, 4 and 5) completely reside in LEO. Two objects (1, 2) have a higher eccentricity and cross into the range of the radar, so that it observes and detects the object regularly.

Table 3.1. Initial orbital parameters of objects.

Object ID	SMA [km]	Ecc. [-]	Inc. [deg]	Dia. [m]
Obj 1	24 730.0	$7.2 \cdot 10^{-1}$	50.3	3.7
Obj 2	26 500.0	$6.6 \cdot 10^{-1}$	64.4	7.1
Obj 3	6840.0	$1.9 \cdot 10^{-3}$	89.0	1.6
Obj 4	7150.0	$2.0 \cdot 10^{-4}$	86.4	5.3
Obj 5	7800.0	$2.0 \cdot 10^{-4}$	52.0	3.9

The MWG is configured to simulate a radar stationed in Germany using mechanical tracking mode, so that at every pass, even at low elevations, the beam is centered on the object. This results in tracklets that have detections with very low SNR to very high SNR, depending on the orbit and the maximum elevation. The radar parameters are given in Tab. 3.2. Using the simplified relations in Equ. 2 each detection has an associated measurement error. The simulation period is two months.
Fig. 3.1 shows an exemplary crossing of an object over the radar station and the analysis of the measurement error using CAT. The pass is represented in the local horizon system using azimuth, elevation and, range information as it passes over the station. The SNR moves between 21 dB and 39 dB, with the highest values around the point of closest approach. At the same time the measurement error reaches a minimum in radial, along-track and cross-track directions, when the SNR surpasses the value of 33 dB. The 33 dB SNR represents the SNR_{ref} reference value where the standard deviation σ of the range and range-rate components stays

Table 3.2. Configuration of the numerical propagator for the tools used.

Parameter	Value
Latitude	50.6°
Longitude	7.1°
Altitude above N.N.	292.9 m
Wavelength	0.225 m
Transmit Energy	0.9 MW
Pulse Repetition Frequency	29.7 Hz
Pulse Duration	1.0 ms
3dB beam opening angle	0.5°

close to constant, as shown in Equ. 2. In this paper the SNR is used as an indicator of the measurement noise. A detection with a $SNR \geq 30dB$ is considered good as the error it holds is comparably low (cp. position error in Fig. 3.1).

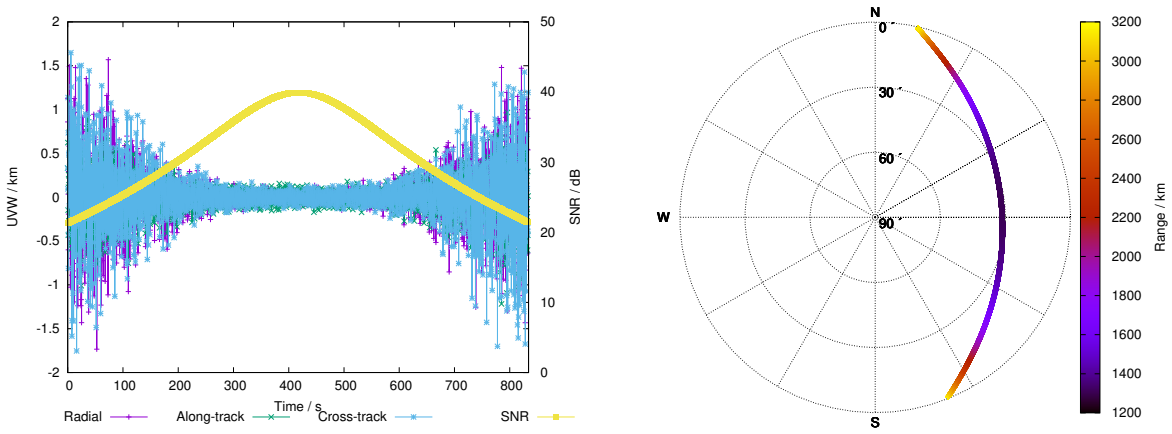

Fig. 3.1. An example pass of an object over the tracking station. On the right showing the local horizon and the distance of the object in km. On the left the noisy position data depending on the SNR.

Multiple tracklets per object are generated for the simulation timeframe of 2 months. Fig. 3.2 shows the total number of tracklets per object that are generated. For the eccentric orbits fewer tracklets are available, as they have an orbital period of 11 h to 12 h hours and maybe in range about once per day on average. The objects that completely reside in LEO have a higher probability of being detected as they have an orbital period of under 2 hours and pass over the station more frequently. On average 6.4 to 7.5 tracklets per day are created.
The tracklets that have been generated are available via the database. PROCOR is subsequently used to manage the OD-backend to process the detections of the 1398 tracklets using different configurations. For statistical OD the WLS and UKF methods are selected. The Gibbs and Herrick-Gibbs IOD methods are used for an analysis of their performance under varying conditions.

4 INITIAL ORBIT DETERMINATION

The IOD algorithms produce the missing velocity vector from three sequential position vectors. The position information are derived directly from the radar measurements as they are available in the local horizon system. The range, azimuth and elevation (RAE) components are transformed into the Earth Centered Intertial (ECI) frame. The Gibbs or Herrick-Gibbs method can be used to derive the missing velocity vector valid for the central position. The quality of the derived velocity vector changes depending on the size of the

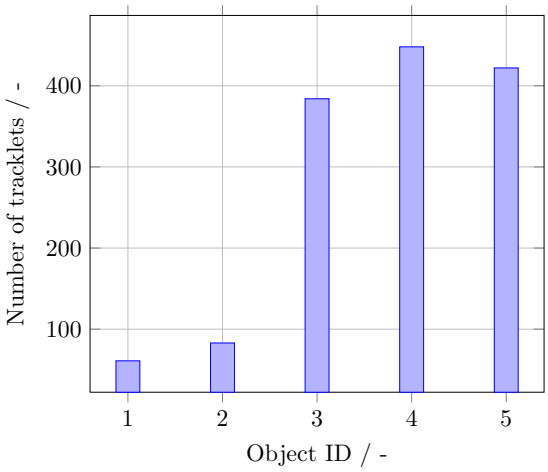

Fig. 3.2. Number of tracklets available per object over the two months simulation period.

observation arc. As shown the generated tracklets are of varying quality, depending on the way the object passes over the radar station. The two months time period of the simulation leads to a variety of passes with different observation arcs and SNR values. For the Gibbs and Herrick-Gibbs methods the impact of the available observation arc and SNR is analyzed in regard of the resulting quality of the velocity vector. Observation arcs from 0.5° to 30° are considered. In addition the analysis has been setup so that the average $SNR \geq 30$ and $SNR < 30$ are discriminated. For all available tracklets the first and the third position vector are selected so that an observation arc with the desired size (e.g. 0.5°) is created, even if the total observation arc available of the tracklet is bigger. Using a sliding window technique the scaled down arc for the analysis is centered around the position vector, which has the highest SNR available. The results of the analysis for each of the defined objects in Tab. 3.1 are shown in Fig. 4.1. The solid and dashed lines indicate the 90th quantile: 90 % of the velocity vectors have a lower error than the line indicates. The mean values are also shown for all cases as a dashed-dotted line. The velocity error on the y-axis is the magnitude of the delta vector in the satellite centered UVW-frame. The delta vector is the computed difference between the *true* velocity vector (available from the MWG) and the derived velocity vector through the IOD algorithms. Generally, both IOD methods show lower errors, as the observation arc increases to about 15°. For good measurements ($SNR \geq 30$) it can be observed that error increases again as the arc increases over the 15° mark when the Herrick-Gibbs method is used. This can be observed for Obj 2, 3 and 4. Even though the average SNR of the chosen three position vectors is above 30dB, the first and last chosen position vectors are in the area where the SNR is below 30 dB and thus hold greater position errors, which are reflected in the derived velocity vector. The radar configuration does not produce detections with $SNR \geq 30$ for Obj 1 and Obj 5. For Obj 3 observation arcs cannot be greater than 15° until the average SNR drops below 30 dB. Overall the Herrick-Gibbs method shows lower errors in all test cases than the Gibbs method. The Gibbs method does not show the behavior where the velocity error increases again, when the observation arc is greater than 15°. Using the Herrick-Gibbs method with good measurements ($SNR \geq 30$) can reduce the velocity error by 2 orders of a magnitude in comparison to the Gibbs method, especially for small observation arcs (cp. Obj 4). The associated velocity errors can be as low as $1 \cdot 10^{-3}$ km /s to $2 \cdot 10^{-3}$ km /s, given optimum observation arcs are used and the quality of the measurements is good.

5 STATISTICAL ORBIT DETERMINATION

In contrast to the IOD the statistical OD methods need an initial state, which is improved using the measurements of a sensor. For further analysis in this paper PROCOR configures the SMART instances to process the same tracklets, which have been used with the IOD algorithms with statistical methods again. The first tracklet of each object is always processed using the Herrick-Gibbs IOD method with optimum settings, as discussed in Sec. 4 in order to derive the first state. Furthermore, when using the UKF the second tracklet is processed using the WLS algorithm to derive a first covariance, which is needed for the UKF. The analysis

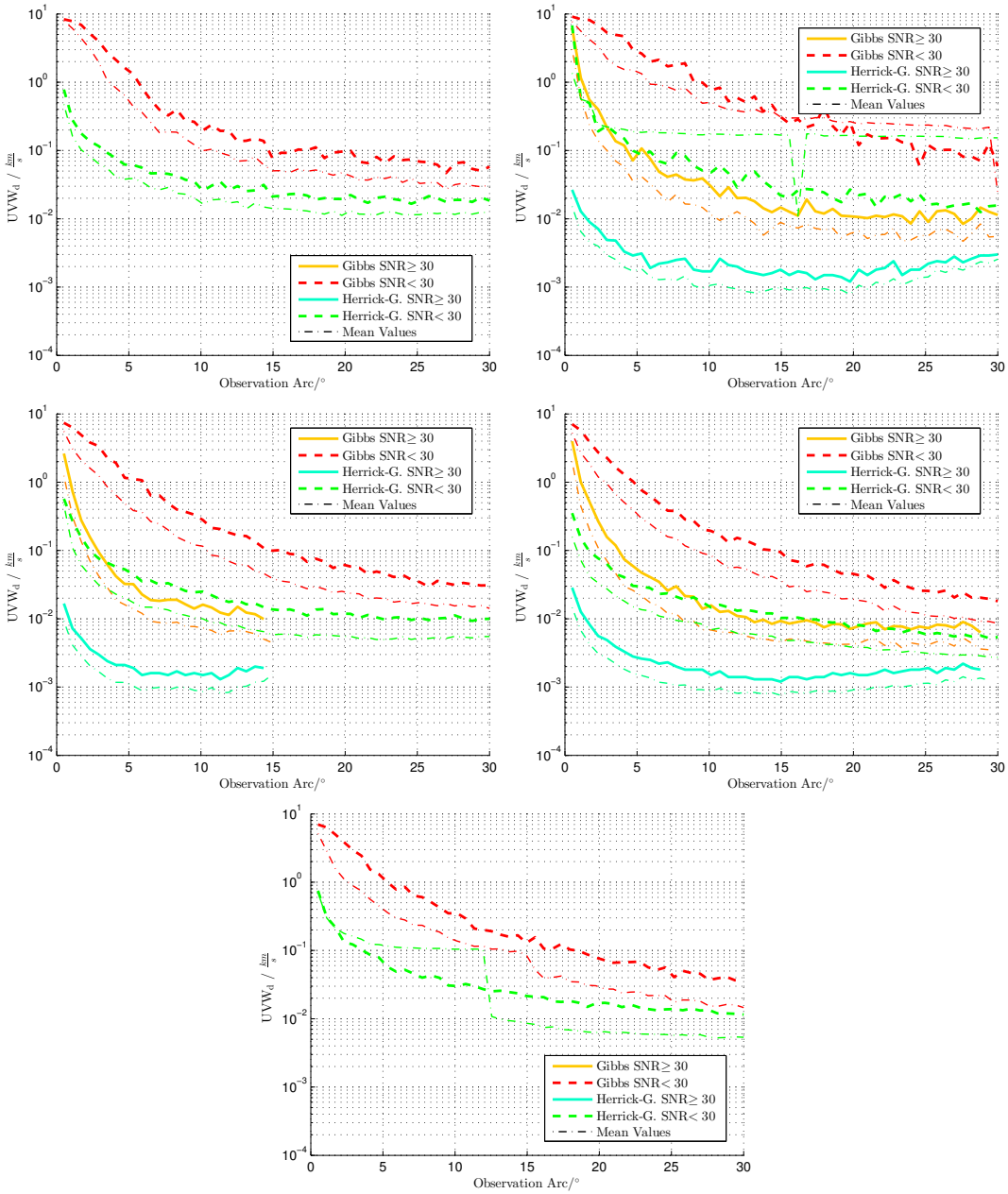

Fig. 4.1. Analysis of results of Gibbs and Herrick-Gibbs IOD methods depending on the observation arc and the SNR. Upper left: Obj 1; upper right Obj 2; center left Obj 3; center right Obj 4; centered below Obj 5.

focuses on the performance of the algorithm as a function of the maximum number of detections per tracklet that are available. When more detections are available a filter is applied. PROCOR manages the selection of the detections so that the time difference between them is the same.

5.1 Weighted Least Squares

The WLS algorithm derives the measurement error used in the differential correction from each detection. Only one tracklet per OD process is used. Thus no fitting over multiple tracklets has been performed. The

magnitudes of the position and velocity error vectors in the satellite centered UVW-frame for each object are shown in Fig. 5.1. The analyzed states have been filtered for the highest available SNR values ($SNR > 30dB$) on the left. For Obj 1, 3 and 5 states with associated measurements below an SNR of 30 dB have also been accepted as there were to few or none at all available (cp. Fig. A.1 in Sec. A). It can be observed that using an increasing number detections improves the accuracy of the produced state. For the part of the analysis where only a few detections ($n < 50$) have been used to determine the state a higher variation and single peaks can be noticed (cp. Obj 1 and 2). The accuracy of these objects with higher eccentricity can reach about 80 m to 350 m position and 0.7 m s^{-1} to 2 m s^{-1} velocity accuracies, given that enough detections per tracklet are available. Obj 3 and 4 show the highest accuracies reaching as low as 18 m to 25 m position and 0.2 m s^{-1} to 0.3 m s^{-1} velocity errors. They reside in low Earth orbit and are observed frequently. Due to their low altitude their measurements have higher SNR values and thus lower measurement noise, which can also be seen in Fig. A.1 showing the histogram of tracklets per SNR bin.

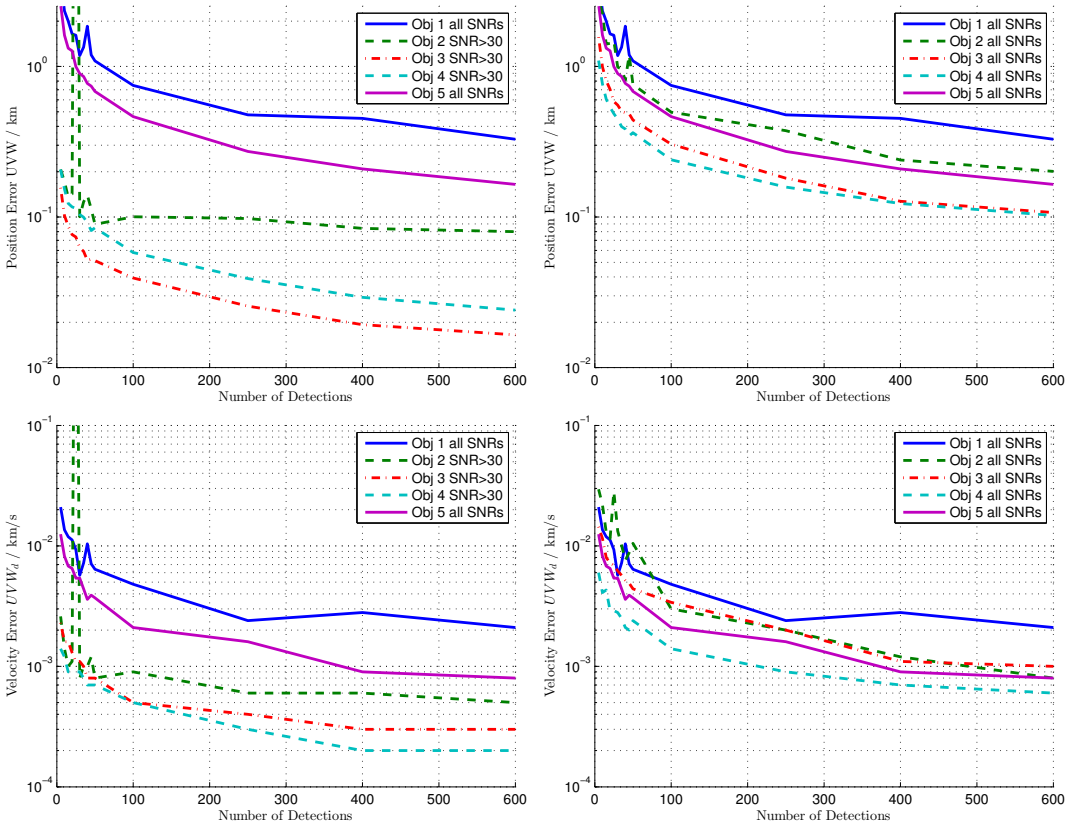

Fig. 5.1. Analysis of the position (top) and velocity (bottom) errors for all objects as a function of the number of detections. The left graphs shows results, which use all state vectors available. The right graphs use a filter on the state vectors, which have been generated from detections that have an $SNR > 30dB$, where possible.

When using all available detections to perform the WLS OD the accuracy of the state vectors is reduced as can be seen on the right of Fig. 5.1. For Obj 3 and Obj 4 the position errors moves up from 18 m to 103 m and 25 m to 102 m, respectively. This is an increase of the error by a factor 4 (Obj 3) and 5 (Obj 4). The same observation can be made for the velocity vector as the error increases by the factor 5. For Obj 2 the error is increased by a factor of 2. Results of Obj 1 and Obj 5 remain the same, as there were no detections available with a $SNR > 30dB$.

5.2 Unscented Kalman Filter

In the implementation the time update of the UKF 13 sigma points χ are created from the current state $\bar{X}$ and covariance matrix P using the unscented transformation [14]:

$$\begin{aligned}
\chi_{0,k-1} &= \bar{X} \\
\chi_{i,k-1} &= \bar{X} + \left(\sqrt{(n+\lambda)\,P_{k-1}}\right)_i \qquad \text{for} \quad i = 1,\ldots,n \\
\chi_{i,k-1} &= \bar{X} - \left(\sqrt{(n+\lambda)\,P_{k-1}}\right)_{i-n} \qquad \text{for} \quad i = n+1,\ldots,2n
\end{aligned} \tag{3}$$

These sigma points, are propagated to the time of the measurement and re-assembled to a state and covariance. Within the unscented transformation a scaling parameter λ is used to define the scatter of the sigma points:

$$\lambda = \alpha^2\,(n+\kappa) - n, \tag{4}$$

with $10^{-4} \leq \alpha \leq 1$ and $\kappa = 3-n$ as stated in [14] and [13], where n is the number of state vector components. The statistical OD analysis is extended to the weighting factor α of the sigma points used in the UKF process to evaluate the optimum setting for different objects and detection numbers. In the analysis the α value has been varied between 10^{-4} to 10^{-3}. Fig. 5.2 shows exemplary results of the analysis for Obj 3 and Obj 4. The UKF does not work with all settings. For these two values of the scaling factor α lead to the lowest position error in the evaluation. For Obj 3 and less then 300 available detections a value of $\alpha = 0.010$ produces the least errors in the test cases. For 200 to 300 detections $\alpha = 0.009$ shows slightly better results, while $\alpha = 0.007$ works best for 300 to 600 detections. For Obj 4 the scaling factor α can be chosen between 0.010 to 0.009 for a number of detections $n < 400$ and $n > 400$ respectively.

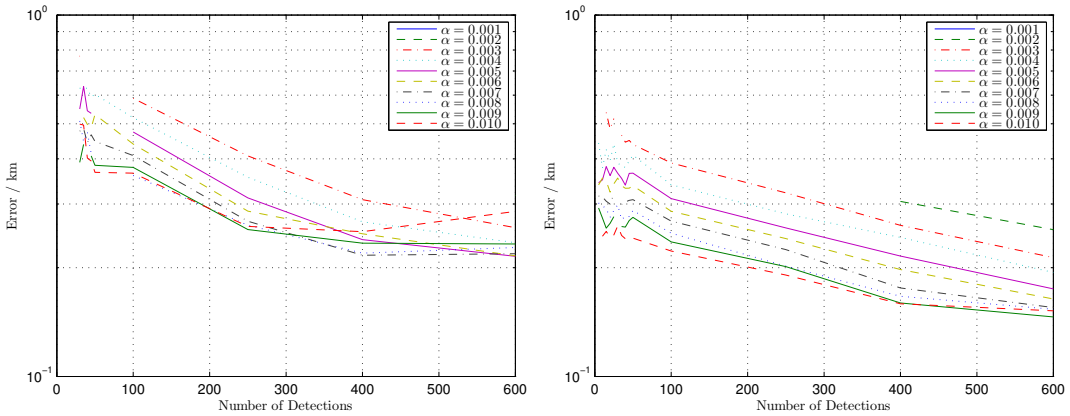

Fig. 5.2. Analysis of the position accuracy as a function of the scaling factor α and the number of detections for the Obj 3 (left) and Obj 4 (right).

For the comparison of the two statistical OD methods Fig. 5.3 shows their performance. While the current UKF implementation shows variation for low detection numbers ($n < 50$) for Obj 3 it also shows better position accuracies than the WLS. When considering Obj 4 for detection numbers $n < 100$ per tracklet the UKF should be preferred. When more detections are available the WLS can be used in these test cases. Please observe that in the case of Obj 4 the accuracy of the UKF OD only improves slightly with an increasing number of detections, from about 250 m to 170 m. Under the same conditions the WLS OD moves from about 1000 m to 100 m. Overall the UKF shows a higher accuracy in the velocity components. Accuracies of $1.9 \cdot 10^{-4}$ km /s to $1.8 \cdot 10^{-2}$ km /s can be reached, while the WLS approach does not drop below $6 \cdot 10^{-4}$ km /s. Please note that not all objects can be analyzed as the current implementation of the UKF in SMART shows short comings, which have to be addressed in future updates. Also in comparison

to Fig. 5.1 in Sec. 5.1 no filtering of the produced states in regards to the associated SNR value of the measurement has been performed.

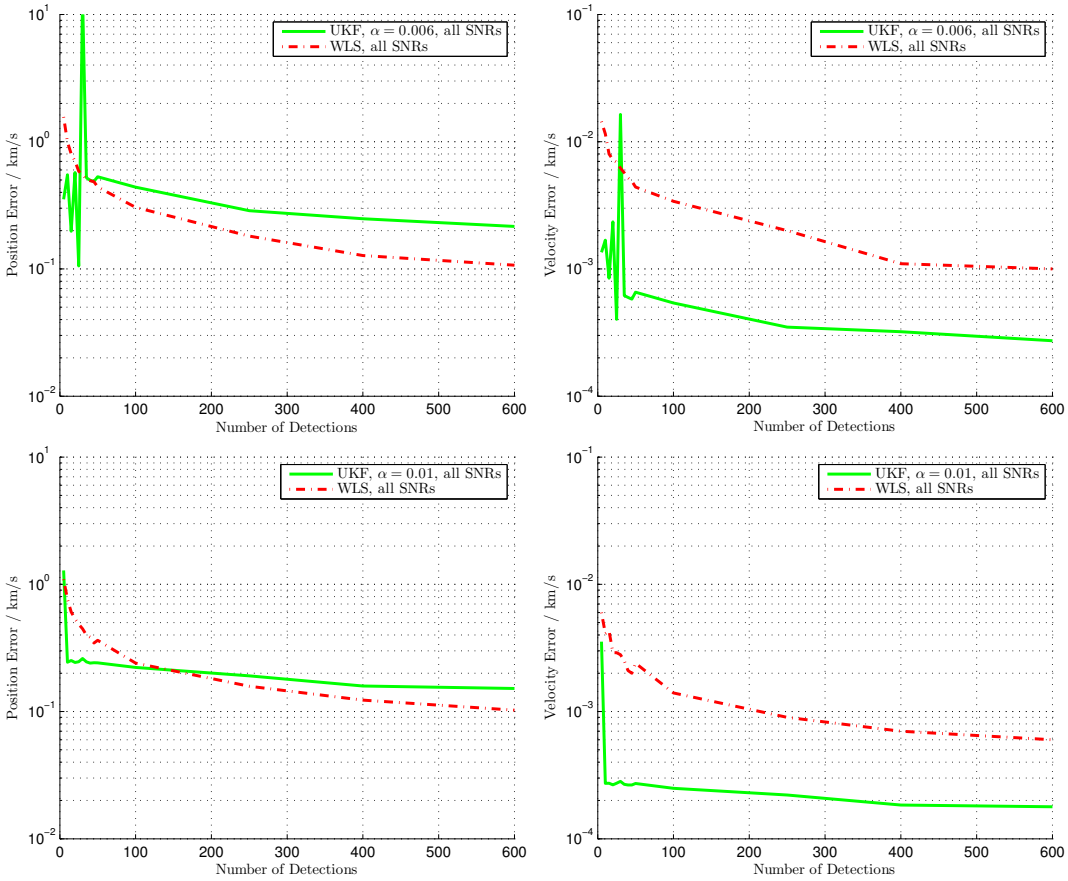

Fig. 5.3. Comparison of the position (left) and velocity (right) accuracy between the WLS and UKF method for Obj 3 (top) and Obj 4 (bottom).

6 CONCLUSIONS AND OUTLOOK

In this paper the architecture of the Radar System Simulator (RSS) software suite has been outlined. The tools involved have been described. The Messwertgenerator (MWG) is used to derive synthetic measurements. With its underlying radar performance model, developed by the Fraunhofer FHR, it is able to simulate mechanical and electrical tracking mode of dish antennas and phased arrays as well as the scanning mode of phased arrays. The tool creates detections that are grouped per objects into tracklets. Each detections holds information on azimuth, elevation, range, and range-rate, as well as an indicator of its quality in the form of the Signal-to-Noise Ratio (SNR). For five test cases measurements have been created using a tracking antenna simulation configured with settings of the Tracking and Imaging Radar (TIRA). The simulation timeframe was 2 months. As a result 1398 tracklets have been created. These tracklets have been processed by different Orbit Determination (OD) methods. The Initial Orbit Determination (IOD) method Herrick-Gibbs produced the best results for all test cases. An optimum observation arc of 15° was found for the chosen setup. The results of the Weighted Least Squares (WLS) statistical OD was tested with regard to the number of detections available for the process. It was found that an increasing number of detections also improves the accuracy of the computed state vectors. The quality of the state vector can further be improved when filtering for detections with high $SNR > 30dB$, which indicates measurements with a low noise level. The Unscented Kalman Filter (UKF) results have been analyzed in regards to the number of

detections and the scaling factor α, which influences the scattering of the sigma points used in the UKF OD process. Preferable α values move between 0.007 and 0.010, depending on the test case and number of detections available. Generally, the UKF shows good position accuracy when a low number of detections are available. However, for the test cases in this paper the WLS shows lower position errors, when the number of available detections increases. Overall the UKF produces the lowest velocity errors. In the future the study will be repeated with a larger number of test cases and different sensor settings. Furthermore, the timeframe of the simulation will be increased, so that more tracklets are available for the analysis. The UKF implementation will be improved so that results are available in all test cases. In future studies comparisons with other statistical OD methods, like the Extended Kalman Filter (EKF) or the Ensemble Kalman Filter (EnKF) can be incorporated. Once optimum settings are found the RSS can be used to study the buildup of an object catalogue with different sensor stations. The impact of more data or an increased resolution of the sensor on the cataloguing back-end can be studied.

7 ACKNOWLEDGEMENTS

The authors would like to thank the DLR, which supports this work under contract AZA 50LZ1404 "Entwicklung eines Radar-System-Simulators". Furthermore, within the contract the Fraunhofer FHR developed the OVER radar performance model, which is an integral module of the MWG.

8 REFERENCES

[1] http://www.esa.int/About_Us/Welcome_to_ESA/ESA_s_Purpose.

[2] https://www.postgresql.org/docs/9.4/static/release-9-4-13.html.

[3] I. A.Gómez, S. A. Vildarraz, C. G. Sacristán, J. M. H. Garnica, C. P. Hernández, M. A. R. Prada, J. U. Carazo, G. M. Pinna, S. Moulin, P. Besso, H. Krag, J. R. Benayas, P. O. Sanz, Á. G. Torrego, A. M. A. Sánchez, N. S. Ortiz, R. D. González, and N. Ortiz. DESCRIPTION OF THE ARCHITECTURE THE SPANISH SPACE SURVEILLANCE AND TRACKING SYSTEM. In *Proceedings of the 7th European Conference on Space Debris*, 2017.

[4] J. P. Arregui, J. Tirado, E. Parrilla, J. Castro, D. Escobar, A. Águeda, N. Sánchez-Ortiz, H. Demir, and H. Krag. ESA's SST DATA CENTRE INTEGRATION. In *Proceedings of 7th European Conference on Space Debris*, 2017.

[5] M. Berry. *A variable-step double-integration multi-step integrator*. PhD thesis, Virginia State University, 2004.

[6] V. Braun. *Providing orbit information with predetermined bounded accuracy*. PhD thesis, TU Braunschweig, December 2016.

[7] V. Braun and A. Horstmann. Networking/Partnering Initiative TU-BS/ESOC (2011 - 2015). Technical report, Institute of Space Systems, 2015.

[8] R. Domínguez-González, N. Sánchez-Ortiz, N. Guijarro-López, P. Quiles-Ibernón, and J. Nomen-Torres. CATALOGUING SPACE OBJECTS FROM OBSERVATIONS: CORTO CATALOGUING SYSTEM. In *Proceedings of the 7th European Conference on Space Debris*, 2017.

[9] H. Fiedler, J. Herzog, M. Ploner, M. Prohaska, T. Schildknecht, M. Weigel, and M. Klabl. SMARTnet – First Results of the Telescope Network. In *Proceedings of the 7th European Conference on Space Debris*, 2017.

[10] S. Flegel. Final Report - Maintenance of the ESA MASTER Model. Technical report, Institute of Aerospace Systems, 2011.

[11] S. K. Flegel. Entwicklung eines Radarsystemsimulators - Program for Radar Observation Vector Estimation (PROVE). Technical report, Fraunhofer FHR, 2015.

[12] T. Flohrer and H. Krag. SPACE SURVEILLANCE AND TRACKING IN ESA'S SSA PROGRAMME. In *Proceedings of the 7th European Conference on Space Debris*. ESA, 2017.

[13] E. Gamper. Untersuchung eines Unscented Kalman Filters zur Orbit Bestimmung. Master's thesis, TU Braunschweig, October 2015.

[14] S. Haykin. *Kalman Filtering and Neural Networks*. Wiley, New York., 2001.

[15] S. Hesselbach. Untersuchung und Implementierung verschiedener Methoden zur Bahnbestimmung. Master's thesis, TU Braunschweig, November 2015.

[16] H. Klinkrad. *Space Debris - Models and Risk Analysis*. Springer, 2006.

[17] P. McCormick. Space Situational Awareness in Europe: The Fractures and the Federative Aspects of European Space Efforts. *Astropolitics*, 13(1):43–64, 2015.

[18] M. Möckel. *High Performance Propagation of Large Object Populations in Earth Orbits*. PhD thesis, Technische Universität Carolo-Wilhelmina zu Braunschweig, March 2016.

[19] B. Reihs. Auswertung von LEO Beobachtungskampagnen. Studienarbeit, TU Braunschweig, Institut für Luft- und Raumfahrtsysteme, Februar 2014.

[20] O. Rodriguez and U. Hugentobler. SPOOK - A Comprehensive Space Surveillance and Tracking Analysis Tool. In *Proceedings of the 7th European Conference for Aeronautics and Space Science*, 2017.

[21] D. A. Vallado and W. D. McClain. *Fundamentals of Astrodynamics and Applications*. Microcosn Press and Springer, third edition, 2007.

[22] H. Wilden, C. Kirchner, O. Peters, N. Ben Bekhti, R. Kohlleppel, A. Brenner, and T. Eversberg. GESTRA-TECHNOLOGY ASPECTS AND MODE DESIGN FOR SPACE SURVEILLANCE AND TRACKING. In *Proceedings of the 7th European Conference on Space Debris*, 2017.

Appendix A SNR HISTOGRAMS

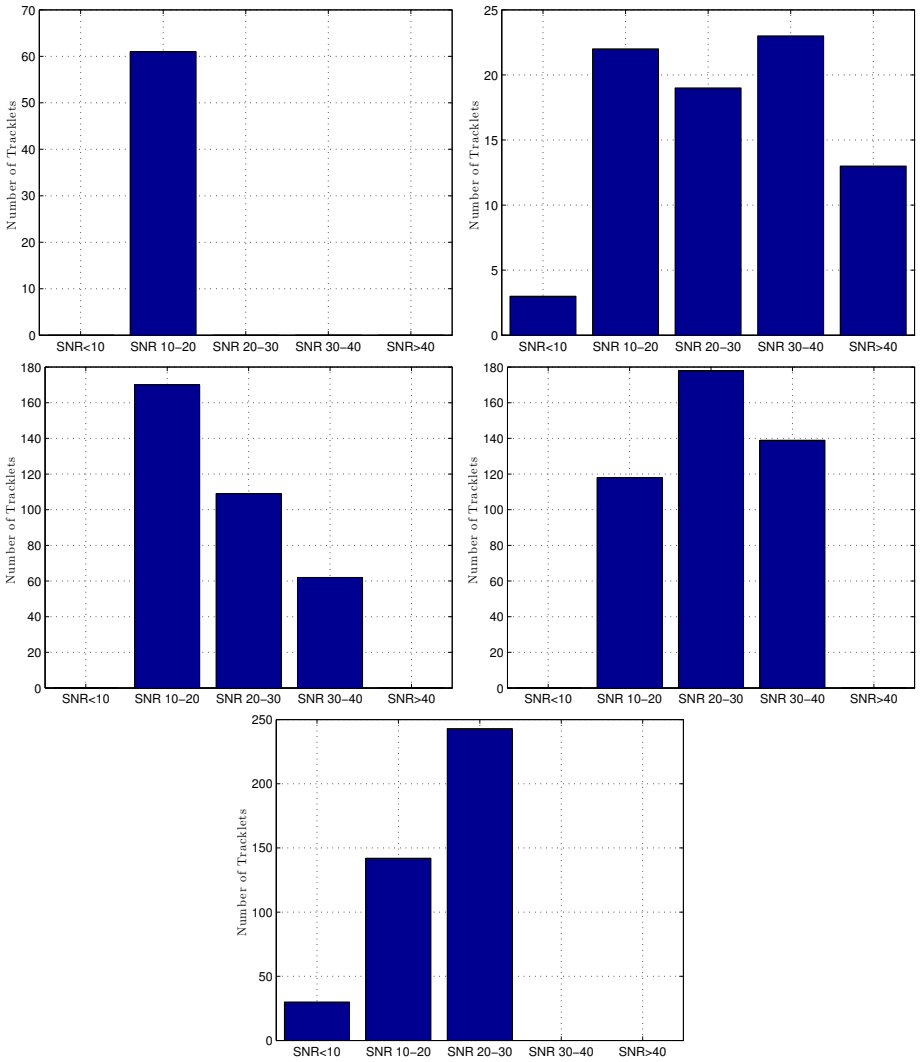

Fig. A.1. Histogram of tracklets in different SNR bins for each object. Upper left: Obj 1; upper right Obj 2; center left Obj 3; center right Obj 4; centered below Obj 5.